β–Cyclodextrin nanosponge hydrogels as drug delivery nanoarchitectonics for multistep drug release kinetics

Roberto Pivato,[a] *Filippo Rossi,*[a] *Monica Ferro,*[a] *Franca Castiglione,*[a*] *Francesco Trotta,*[b] *Andrea Mele*[a,c]

[a] Department of Chemistry, Materials and Chemical Engineering "G. Natta", Politecnico di Milano, Piazza L. da Vinci 32, 20133 Milano, Italy.

[b] Department of Chemistry, University of Torino, Via Pietro Giuria 7, 10125 Torino, Italy.

[c] Istituto di Scienze e Tecnologie Chimiche (SCITEC-CNR), Via A. Corti 12, 20133 Milano, Italy.

KEYWORDS. hydrogel, controlled release, β-cyclodextrin nanosponge, NMR spectroscopy, diffusion.

ABSTRACT

The reaction of β-cyclodextrin with suitable bi-functional crosslinkers (such as carboxylic acids dianhydrides) provides 3D, nanoporous polymers referred to as cyclodextrin nanosponges (CDNS). The swelling ability of many CDNS can be exploited to confine small active molecules – such as drugs – in the resulting hydrogel, thus providing drug-loaded CDNS hydrogels. This raised an increasing interest towards CDND hydrogels as biomaterials for controlled drug delivery due to their nontoxicity, biocompatibility and biodegradability. The release kinetics of a drug carrier is often influenced by the physical and chemical properties of the hydrogel nanoarchitectonics and the drug-polymer interactions across the 3D network. A deep understanding, at the molecular level, of the mechanisms underlying drug dynamics in the hydrogel polymer matrix and the relation with the macroscopic release kinetic is a key step for a rational design of delivery systems.

In this study, nanosponge-hydrogels are prepared by cross-linking β-cyclodextrin with pyromellitic dianhydride and swelling the corresponding polymer loaded with the anti-inflammatory drug piroxicam.

The translational dynamics of the small drug in the optimized hydrogel formulation is investigated by ^{1}H high resolution magic angle spinning (HR-MAS) NMR spectroscopy at variable observation times. The micro-scale results, compared with *in vitro* release kinetics performed on a much longer time-range, reveal a continuum Fickian dynamics of the drug within the 3D polymer network. The multistep prolonged release of the drug is influenced in a combined mode by the polymer nanoarchitectonics with adsorption of the drug-to-polymer network and β-cyclodextrin-drug complex formation.

INTRODUCTION

β-Cyclodextrin (β-CD) is the most popular and used cyclic oligomer of amylose, characterized by seven *D*-glucopyranose units linked together to form a macroring by α-1,4 glycosidic bonds. The resulting molecule has a truncated-cone shaped cavity with marked hydrophobic characteristics and a hydrophilic external surface. The hydrophobic void can host apolar molecules of suitable size by the establishment of a stoichiometric, non-covalent inclusion complex. A plethora of CD host-guest complexes have been formulated, characterized, patented and/or exploited in a broad range of applications, spanning from pharmaceutical formulations to cosmetics, from environmental remediation to chiral stationary phase for chromatography. All of these aspects of CD chemistry have been massively documented in the last decades.[1-3]

From a different viewpoint, cyclodextrins can be also considered as monomers capable to generate three-dimensional polymeric architectures via the functionalization of the numerous reactive OH groups present on the external surface. In particular, each glucopyranose units has, in principle, two secondary OH groups and one primary OH amenable of condensation reaction with a bi- or multifunctional reactant. In the case of β-CD this leads to 21 potential reactive sites per monomer. If the polymerization is carried out by using cross-linking agents such as activated derivatives of bi-carboxylic acids (pyromellitic anhydride (PMA), EDTA dianhydride, or synthetic equivalents of carbonic acid), a nanoporous and highly entangled 3-dimensional polyester architecture[4-6] is obtained, commonly referred to as cyclodextrin nanosponge (CDNS). It is important to remark, at this stage, that the polymer porosity is provided by two different types of voids inside the polymer: *i)* the pores naturally formed during the random cross-linking process (voids I) and *ii)* the macrocycle of the cyclodextrin units (voids II), already present in the

monomeric CD. Different and versatile types of CDNS can be prepared by suitable choice of the cross-linker, the CD/cross-linker molar ratio, the reaction conditions.[7] A general scheme of the types and features of CD-based nanosponges is sketched in Scheme 1.

CDNS find several scientific and technological applications in areas such as, agriculture,[8] cosmetics, gas-carrier,[9] pharmaceutical chemistry[10,11] and drug delivery[12,13]. The latter is one of the most relevant application due to the different formulations easily obtainable by tuning the preparation conditions, such as nanoporous nanoparticles with few nanometer wide spherical cavities, or by exploiting the swelling propertied of many CDNS, thus providing CDNS hydrogels able to encapsulate small active ingredients and release them in a controlled way. A paradigmatic example, which is also the object of the present work, is represented by CDNS obtained via cross-linking of β-CD with PMA and easily converted in hydrogel by swelling with water solutions (Fig. 1). The CDNS hydrogels obtained in that way are chemical gels with permanent covalent bonds between cyclodextrins units, and generally characterized by a high capacity of encapsulating small molecules and various type of cross-linkers.[14] In the last few years our group has synthesized and characterized by spectroscopic techniques[15,17] a large repertoire of CDNS hydrogels, and some of them have been proposed as delivery systems suitable for drug release induced by external stimuli.[18,19]

In the general scenario of engineered hydrogels,[20-23] antimicrobial biometallo-hydrogels base on amino acids coordinated self assembly[24], injectable hydrogels based on the self-assembly of collagen proteins with a gold-biomineralization-process[25], have been synthesized and proposed as localized drug delivery systems. CDNS hydrogels can also be considered smart materials as they can have pH dependent swelling degree[15] or other tunable variables affecting the degradation kinetics.

Despite the variety of polymer hydrogels proposed as drug carriers,[26,27] obtaining an optimal delivery system of long/short-acting drugs and macromolecular drugs requires as primary step a deep understanding, at a molecular level, of the drug motion within the polymer network and its relation with the hydrogel structure and morphology.[28]

In this context, it is often assumed that drug transport and release in swollen hydrogels obey the Fick's laws of diffusion, and can be adequately described using, or slightly modifying, the equations adopted to describe Gaussian motion.[29,30] Although this assumption may hold true in isotropic solutions and several hydrogels, growing evidence of anomalous,[31,32] non-Gaussian diffusion in a variety of "soft" and porous materials[33] raises a number of questions about its mere applicability. Indeed many phenomena that occur only at the molecular level, such as drug-polymer (*adsorption*) and drug-drug (*aggregation*) interactions[34-36] can be held responsible for anomalous mass transport in gels and must be taken into consideration through the exploitation of appropriate mathematical models supported by experimental data to assess the release mechanism. To date, numerous models of drug release from polymers and hydrogels have been proposed in the literature, including a simple diffusion model, like the classical Higuchi equation,[37] and more complex mechanistic models[38-42] essentially based on *i)* obstruction effects, *ii)* free volume theory,[43] and *iii)* hydrodynamic theories[44] which take into account the hydrodynamic interactions present in the whole system. Moreover, additional and more specific modeling strategies accounting for the effects of electrostatic interactions, pH and ionic strength have been proposed to describe the diffusion of ions in agarose gels.[45]

In CDNS hydrogels, the encapsulated solute is likely to experience interactions such as hydrogen bonding and hydrophobic interactions with the CD units and/or the covalent bridges established by the cross-linkers with the CD during the polymerization. Additionally, CDNS

polymer architecture is designed so as to possess different sized sites for binding small drugs. These factors are expected to interfere with the random motion of the solute, thus affecting its diffusivity.

In this work, we prepared a suitable model system of CDNS hydrogel loaded with a small molecule to study the type of motion of the solute in the confined scaffold and to compare the diffusion data with the macroscopic release kinetic. The polymeric hydrogel here considered is the CDNS obtained from pyromellitic dianhydride (PMDA). The hydrogel is loaded with the model active pharmaceutical ingredient piroxicam sodium salt (PRX) (scheme 1) in order to obtain a drug-loaded CDNS hydrogel to be investigated as controlled drug delivery system. The choice of PRX as probe for the assessment of the type of motion was dictated by two reasons: *i)* the 1:1 inclusion complex of monomeric β-CD and PRX is a registered pharmaceutical formulation commonly available as a prescription. The characterization of the complex[46] is well known and it is part of the scientific background of the group, thus PRX can be considered as a benchmark. *ii)* PRX belongs to the oxicam class of nonsteroidal anti-inflammatory, analgesic, antipyretic drugs (NSAID) which are used clinically for the treatment of various arthritic conditions, fever and pain. The physico-chemical characterization of its behavior in CDNS hydrogels adds value to the study in view of new formulations. The main focus of this work relies upon the dynamics of PRX encapsulated in the CDNS polymer network and the comparison of diffusivity with release data.

Within the broad repertoire of physical methods[47] for the structural characterization of gels and for the investigation of solute-polymer interactions, we chose NMR spectroscopy to measure the solute diffusivity in the gels via Pulse Gradient Spin Echo (PGSE) methods, an experimental noninvasive technique widely used for the investigation of the translational motion of small

molecules in liquid solution[48-50] and hydrogel systems.[31,32,51,52] To best apply this methodology, high resolution (i.e. liquid-like) spectra are needed even in soft materials, where the high viscosity is expected to cause severe line broadening of the NMR lines, thus rendering the spectra completely useless. The High Resolution Magic Angle Spinning (HR-MAS) NMR probehead, designed to spin the sample up to 4 kHz at the magic angle θ=54.7° and to apply magnetic field gradients along such axis, have been used to efficiently reduce the resonance line broadening effects caused by chemical shift anisotropy, dipolar interactions, and magnetic susceptibility differences intrinsic in semisolid materials. The combined and systematic use of PGSE methods under HR-MAS condition has been reported as a powerful method to measure diffusion rates in soft materials.[53] Furthermore, since diffusion can be evaluated at variable observation time,[31] information regarding the motion regime in the milliseconds time-scale, and the influence of the hydrogel network on drug diffusivity are evaluated. The NMR results are finally compared with the macroscopic release kinetics.

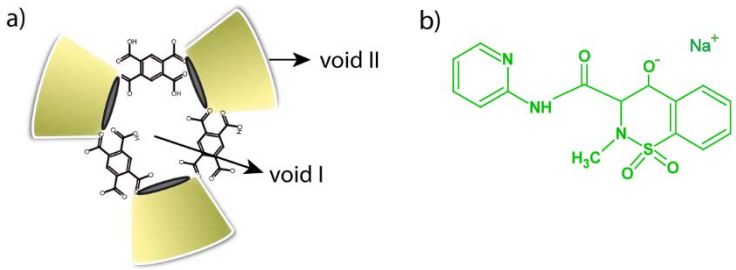

Scheme 1. a) Schematic representation of of CD-based nanosponges crosslinked with PMDA. b) Chemical structure of piroxicam sodium salt.

EXPERIMENTAL SECTION

Materials. β-CD nanosponge crosslinked with PMDA in molar ratio 1:3 was produced according to the procedure described by Trotta *et al.*[4,54] Piroxicam (4-Hydroxy-2-methyl-3-(pyrid-2-yl-carbamoyl)-2H-1,2-benzothiazine 1,1-dioxide) was purchased from Sigma-Aldrich (purity ≥ 98%) and converted in sodium salt by titration with NaOH/H_2O solution. A physical mixture composed of 50 mg of nanosponge and 20 mg of drug was prepared, after which a solution composed by:

i. 400µl of deuterated water;

ii. 10% w/w of sodium carbonate Na_2CO_3

was also prepared and pipetted over the physical mixture. Samples were left for 4 days to swell at room temperature to obtain the drug loaded hydrogel (PRX@CDNS) before analysis. The schematic representation of the entire experimental protocol is shown in figure 1. The initial drug concentration in gel is indicated as C_g. Several liquid solutions composed by piroxicam dissolved in D_2O (PRX@D_2O) at concentrations (C_1=0.003, C_2=0.006, C_3=0.015, C_4=0.033, C_5=0.06, C_6=0.15 M) were also prepared for NMR analysis. The TSP (3-(trimethylsilyl)-propionate, sodium salt) was added as chemical shift reference.

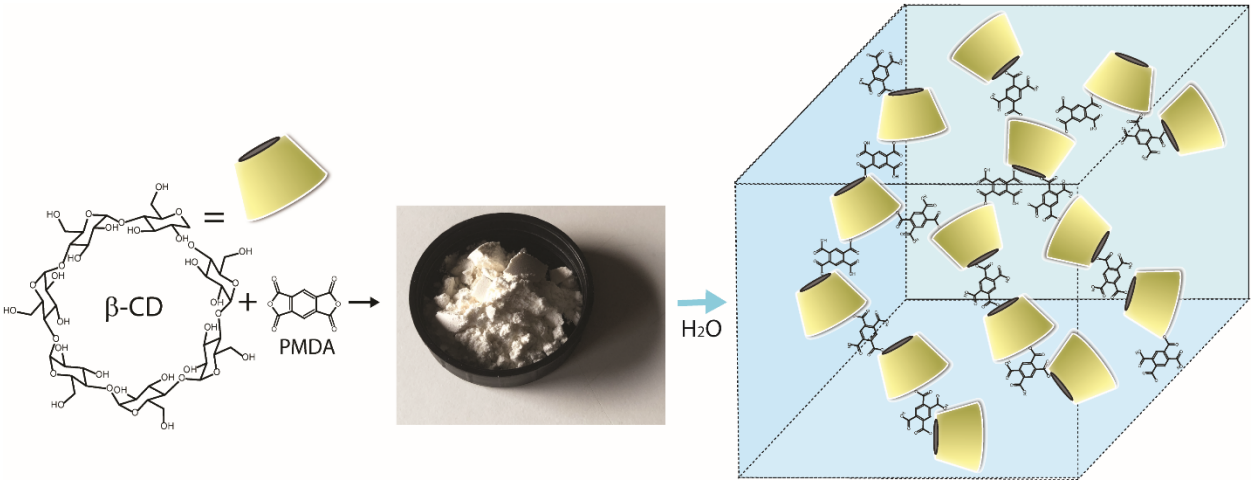

Figure 1. Schematic representation of the β-CDNS synthesis and swelling with H_2O to form the hydrogel.

Swelling degree (*Sw*). The swelling studies were carried out by immersing a dried β-CDNS sample of weight (w_d) in water solution and an aliquot of Na_2CO_3 (10% w/w) was added. The sample was left to swell at room temperature for four days. Afterwards, the weight of the hydrated polymer (w_h) was measured. The swelling degree was computed as percentage according to:

$$\%Sw = \frac{w_h - w_d}{w_h} * 100 \quad (1)$$

Drug loading (*DL*) and entrapment efficiency (*EE*). The drug loading and entrapment efficiency of PRX@CDNS were determined according to the following procedure: *1)* 20 mg of PRX were dissolved in 400 μL of water, *2)* 50 mg of β-CDNS and 10% w/w of Na_2CO_3 were further added to the drug-in-water solution, *3)* the sample was left for 24h, under stirring at room temperature, to obtain the drug loaded β-CD NSs. *4)* After 24 h, the mixture was centrifuged to obtain a layer of water-bound material and free unabsorbed water. These two layers were divided and freeze dried, and then their amounts were determined. The encapsulation efficiency, and loading capacity expressed in percentage were calculated as follows:

$$\text{Encapsulation Efficiency (EE\%)} = \frac{(W\ (total\ drug\ added) - W(free\ drug))}{W\ (total\ drug\ added)} * 100 \quad (2)$$

$$\text{Loading capacity (LC\%)} = \frac{W\ (encapsulated\ drug)}{W\ (CDNS\ added)} * 100 \quad (3)$$

Scanning Electron Microscopy (SEM). SEM images of piroxicam and PRX@CDNS were recorded on a Cambridge stereoscan SEM S-360 instrument with different resolution. The

following parameters were used: High voltage: 10 kV, Tilt: 0.00. The hydrogel sample PRX@CDNS, prepared following the procedure described in 2.1.1, was freeze-dried then coated with a thin layer of palladium/gold and carbon cement was used as adhesive.

Drug Release kinetics. CDNS loaded with PRX and swollen with water were prepared according to protocol 2.1.1. The hydrogel was submerged in 2ml of deionised water at room temperature. At defined time intervals, 500 μL of eluate have been collected and 500μl of deionised water have been added to the release medium to avoid mass transfer equilibrium between the hydrogel and the surrounding environment. Samples have been collected every hour for 9 hours, then at 24h, 32h, 48h, 56h, 72h and 80h. The amount of released PRX was measured by UV-vis absorption at λ = 204 nm. The overall release experiments were performed in triplicate for each time point.

NMR Spectroscopy. The ^{1}H spectra of the hydrogel sample were recorded on a Bruker DRX spectrometer operating at 500 MHz proton frequency equipped with a dual $^{1}H/^{13}C$ HR-MAS probe head for semi-solid samples. The gel was loaded in a 4 mm ZrO_2 rotor containing a volume of about 12μL. A spinning rate of 4 KHz was used to eliminate the dipolar contribution.

The ^{1}H NMR spectra of the liquid sample were recorded on a Bruker Avance I 500 spectrometer operating at 500.13 MHz proton frequency equipped with a QNP four nuclei switchable probe. For the sake of clarity, the NMR experiments carried out on liquid solutions contained in the normal 5 mm glass tubes and by using the liquid NMR probe, will be referred to as HR spectra. This is done to avoid any misinterpretation of HR-MAS NMR and HR NMR data.

PGSE NMR experiments were performed on the liquid and gel samples. The BPP-LED pulse sequence was used to reduce eddy current. The duration of the magnetic field pulse gradients δ, and the diffusion times Δ parameters were optimized in every experiment for each sample in

order to obtain complete dephasing of the signals with the maximum gradient strength. For the hydrogel sample variable observation time experiments were performed varying t_d in the range 0.03-0.11 s which correspond to δ= 1.3-3 ms. A single PGSE experiment at a fixed observation time t_d=0.02s was acquired on the PRX@D_2O sample. A pulsed gradient unit capable of producing magnetic field pulse gradients of 53 G·cm^{-1} was used. Pulse gradients were incremented from 5 to 95% of the maximum gradient strength by a linear ramp in 32 steps. A ^{1}H-^{1}H COSY experiment was recorded on the PRX@D_2O liquid sample with 8 transients over 2048 (t_2) x 256 (t_1) complex data points. The temperature was kept constant at 305 K for all the experiments.

NMR-diffusion theory. The dynamic properties of the PRX drug in CDNS nano-porous network are investigated by diffusion-NMR (dNMR) methods.[48] The experimental technique is based on the application of strong additional (to the external B_0) field gradients along a defined direction (usually *z* or z_M in the MAS set-up) for a short time interval δ.

The main information provided by this technique are contained in the attenuation of the signal intensity $I(q,t_d)$ which is related to the molecular mean square displacement (MSD), $< z_M^2 >$, according to the equation (2):

$$I(q, t_d) = I_0(0, t_d) e^{-\frac{1}{2} q^2 \langle z_M^2 \rangle} \qquad (4)$$

where $q = (\delta \gamma g)/2\pi$, γ is the giromagnetic ratio of the observed nucleus, g the gradient intensity. The time delay, t_d, in the milliseconds time scale, is the selected observation time of the experiment, therefore, $< z_M^2 >$ is the squared distance travelled by the molecule at time t_d. Accordingly, several experiments with variable observation times t_d allow us to follow the evolution in time of the molecular MSD, hence the motion regime.

In general, the mean square displacement as a function of time can be expressed through a power law (Eq. 3):

$$\langle z^2(t_d)\rangle = 2D' t_d^{\alpha} \quad (5)$$

where *D*' is a generalized diffusion coefficient and the parameter α is the diffusion exponent, its numerical value can be determined through a log-log plot of $< z_M^2 >$ *versus* t_d as the slope of the linear regression.

The value of α defines distinct motion regimes: if α<1, a sub-diffusion regime takes place, while for α>1, super diffusion phenomena occurs.[55,56] Fickian motion, usually observed in isotropic systems corresponds to α=1 and the constant *D'* is then the molecular diffusion coefficient *D* (m^2/s). Accordingly, eq. 4 becomes the well-known Einstein equation (Eq. 6):

$$\langle z^2(t_d)\rangle = 2D t_d \quad (6)$$

in which the molecular mean square displacement increases linearly with time.

RESULTS AND DISCUSSION

β-CDNS Swelling. β-CDNS are able to absorb a large amount of water giving rise to the formation of hydrogels. The percentage of swelling reached by β-CD nanosponge crosslinked with PMDA was 830% in average.

PRX@CDNS loading and entrapment efficiency. The drug loading and entrapment efficiency were 32.9% and 79.8%, respectively. These values are among the highest reported in literature[57] for drug-loaded CDNS. The high entrapment efficiency may be ascribed to the complex β-CDNS polymer nanoarchitectonics consisting of voids (I) of the CDNS and voids (II) of β-CD.

β-CDNS Morphology. SEM microphotographs of piroxicam and PRX@CDNS formulation are shown in figure 2.

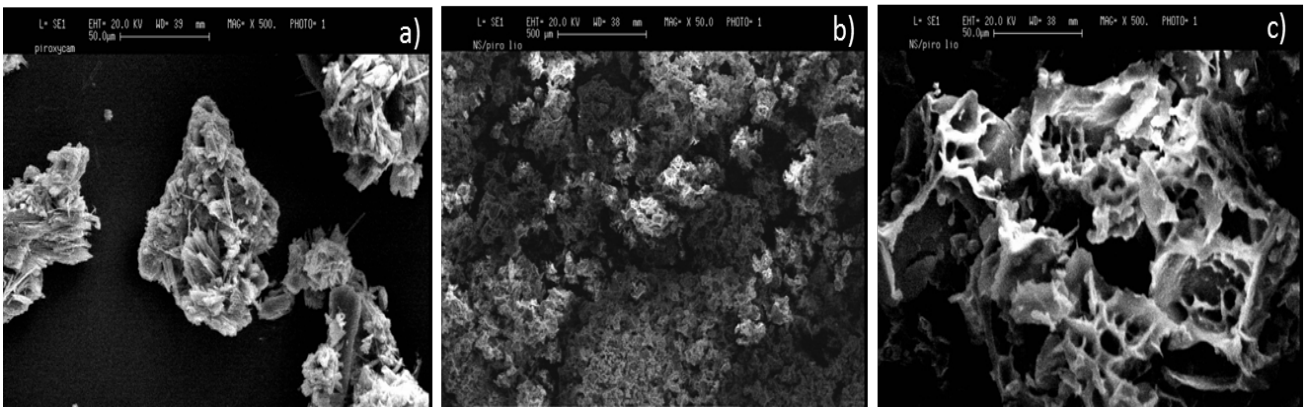

Figure 2. SEM images of PRX a) and PRX@CDNS. b) 50x c) 500x.

The images (b and c) clearly show the porous morphology of the nanosponge material with interconnected internal cavities of different dimensions. Figure 2a shows the typical aspect of the morfology of piroxicam cristals. Figure 2c, at the same magnification level, shows the sponge-like architecture of the polymeric scaffold with no apparent residual clusters of crystalline piroxicam. The freeze-drying procedure carried out on the piroxicam loaded CDNS hydrogel does not lead to separation of piroxicam and re-crystallization. This is consistent with a dispersion of piroxicam in the nanosponge/β-cyclodextrin cavities. However, the formation of large and amorphous aggregates of piroxicam cannot be ruled out. Overall, either the entrapment in the nanosponge, or the alternative formation of piroxicam amorphous aggregates positively affects the drug bioavailability.

NMR Spectroscopy. ^{1}H High Resolution (HR) NMR Spectroscopy is a valuable tool to study structure, aggregation phenomena and dynamics of small molecules dissolved in D_2O solution. When passing from isotropic, non-viscous water solutions to highly viscous soft materials such as hydrogels, the HR-MAS technology is the ideal approach to obtain highly defined NMR spectra of the molecules confined inside the soft matter. The use of HR-MAS NMR allowed to

obtain highly defined NMR spectra of molecules inside soft materials, such as gels. This enabled the investigation of host-guest interactions together with the dynamic properties of small mobile drugs loaded in the nanoporous polymer matrix. The key feature of the HR-MAS NMR approach is the decoupling of the spectroscopic response of the polymer – which is filtered out – and that of the pharmaceutical ingredient which is entrapped but still retains a sufficient degree of mobility to give rise to a high resolution spectrum. The NMR results concerning structure and dynamics of PRX in solution and gel phase are discussed below. The NMR section is divided in two parts. The first one will deal with the possible formation of inclusion complexes of PRX with the CD units of the CDNS polymer, *i.e.* the possible interaction of PRX with voids II, the second one will discuss the dynamic behaviour of PRX inside the hydrogel. We remind here the notation used: PRX@D_2O stands for the NMR analysis of a deuterated water solution of PRX by using solution state NMR analyses. PRX@CDNS stands for the HR-MAS NMR investigation of PRX confined in the hydrogel.

PRX@D_2O and PRX@CDNS Structure

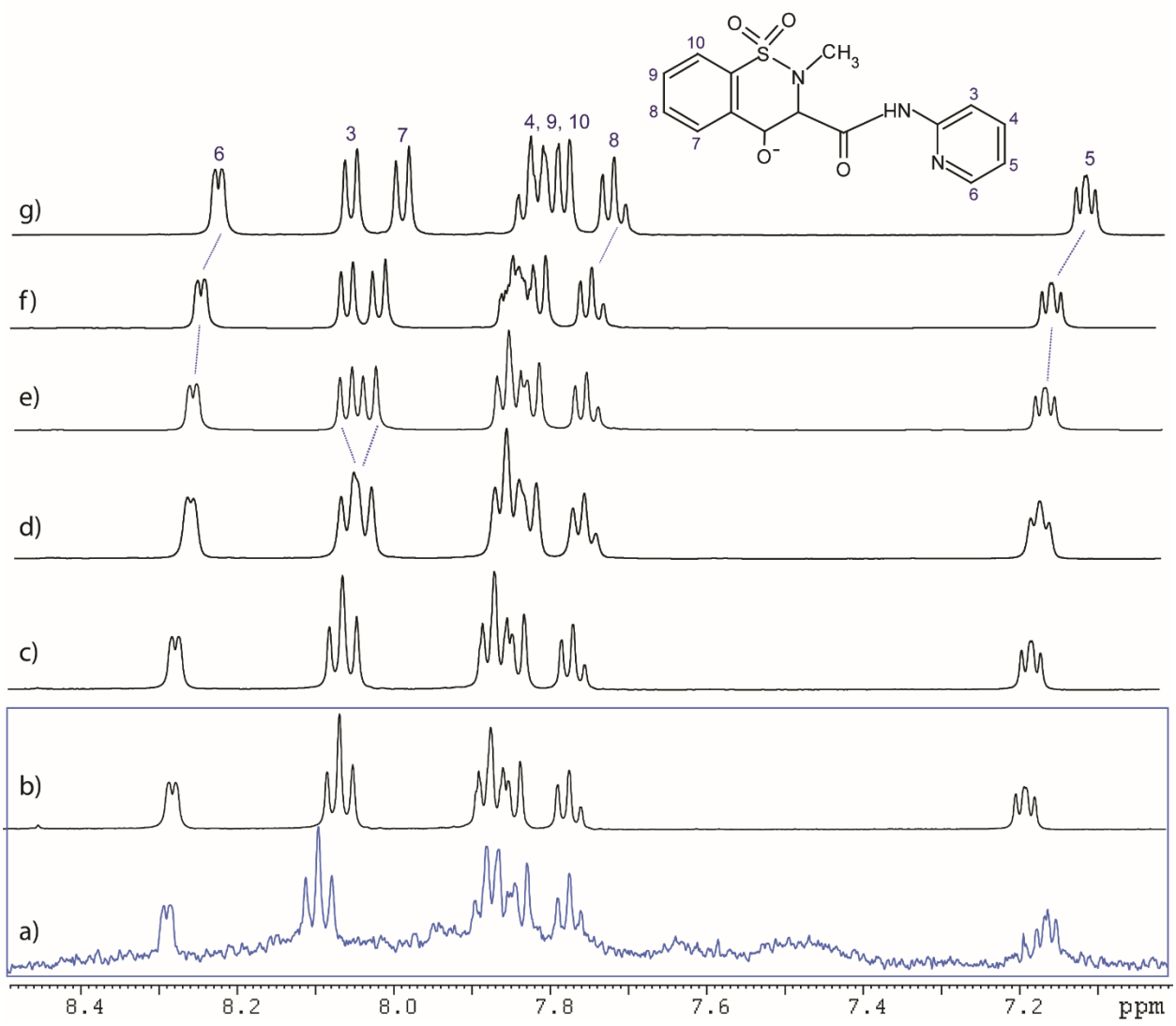

Figure 3. a) ^{1}H HR-MAS NMR spectrum expanded aromatic region (7.0-8.5 ppm) of PRX loaded in CDNS. **b-g)** ^{1}H HR spectra of PRX dissolved in D_2O at different concentrations, b) C_1=0.003M, c) C_2=0.006M, d) C_3=0.015M, e) C_4=0.033M, f) C_5=0.06M, g) C_6=0.15M M. The molecular structure and resonances assignment is also reported. It is important to remark that trace a) corresponds to the NMR spectrum of PRX in the hydrogel obtained under HR-MAS conditions i.e. PRX@CDNS, while spectra b-g) correspond to the solution state NMR spectra of PRX dissolved in D_2O obtained with conventional NMR probe for liquids i.e. PRX@D_2O.

The expansion of the ^{1}H HR-MAS NMR spectrum of PRX@CDNS hydrogel polymer is reported in figure 3a, along with the reference ^{1}H spectra of the drug dissolved in D_2O solution (PRX@D_2O) at several increasing drug concentrations (3b-3g). The spectra, for all the studied concentrations, show well resolved resonances for the aromatic and N-methyl protons except for H4, H9, H10 which form an overlapped multiplet. The spectral region between 5 and 0 ppm is not reported (see SI1). Suffice it to mention that signal assignable to the residual water was a sharp single line, thus indicating a fast exchange between free and bound water on the NMR time scale.

First of all, before discussing in details the comparison between PRX@CDNS and PRX@ D_2O, it is important to observe the effect on the spectral lines of a change in the concentration of the drug dissolved in water. Indeed, a remarkable shielding of all the aromatic and the N-methyl protons ($\Delta\delta$) with increasing PRX concentration is observed. The results for the highest (C_6) and lowest (C_1) drug concentrations are summarized in table 1. The chemical shift changes ($\Delta\delta$) are in the range 0.03-0.06 ppm for all protons except one (H8-aromatic ring) showing a greatest difference of 0.63 ppm. A progressive chemical shift variation with drug concentration, due to a change in the local chemical environment or magnetic fields, is an indicator of aggregation phenomena in solution. It is well assessed that model aromatic compounds show the tendency to aggregate by establishing π-π dimers or superior oligomers.[58,59] This phenomenon has been observed, using ^{1}H NMR, for several aromatic drugs in aqueous solution.[60] The reported $\Delta\delta$ can be interpreted with the formation of small PRX aggregates such as dimer o trimers and even large ones due to non-covalent π-π stacking interactions in water solution.

Table 1. Chemical shift (δ) of PRX dissolved in D_2O solution (0.15-0.003 M), and PRX confined in CDNS (0.15 M).

Sample				Chemical shift (δ ppm) of PRX protons					
	H6	H3	H7	H4	H9	H10	H8	H5	N-Me
PRX@D_2O C_6	8.22	8.05	8.00	7.82	7.77	7.77	7.14	7.11	2.82
PRX@D_2O C_1	8.28	8.07	8.07	7.87	7.84	7.85	7.77	7.18	2.88
PRX@CDNS C_g	8.28	8.09	8.09	7.88	7.83	7.84	7.77	7.16	2.88

The HR-MAS spectrum PRX@CDNS shows well resolved lines of the drug molecules, comparable with the HR spectra (3b-3f), while CDNS polymer, due to the slow mobility of the 3D network, is not observed. A comparison between the HR-MAS spectrum (trace a) and the reference high resolution spectra (trace b-f) shows that the former has the most similar spectral features and chemical shifts (reported in table 1) for protons H6, H8 and N-Me to the lowest concentration liquid sample C_1 and C_2, thus indicating that the effective drug concentration in gel phase is much lower than the initial loading C_g. A large amount of the drug is not free in the gel phase due to drug-to-polymer adsorption and/or drug-βCD complex formation which reduces the amount of molecules available for aggregation. This findings are similar to previous results on sodium fluorescein (SF), a drug-like molecule loaded in agar-carbomer (AC) hydrogels.[35] In that case, broad NMR signals are observed for fluorescein dissolved in water solution, while well resolved lines appear in the gel phase even at high SF concentration. This findings showed that SF was likely to interact with the three dimensional polymeric backbone through an adsorption mechanism.

A closer inspection of the HR-MAS *vs* HR spectrum (panel a-b) reveals that in gel phase protons H3 and H7 experience a downfield shift and H8 an upfiled shift of 0.02 ppm. These changes are probably due to drug/βCD complex formation via incapsulation of PRX in the hydrophobic cavity of the βCD monomers of the CDNS (voids II). The presence or not of inclusion phenomena leading to non-covalent host-guest complexes between PRX and the cyclodextrin units within the CDNS deserves attention. It is known that PRX forms stable 1:1 inclusion complex with monomeric β-cyclodextrin in D_2O solution.[46] The question is whether or not the formation of the inclusion complex occurs even in the nanosponge, where CD is part of a covalent polymeric backbone and it is not present as free monomer. In the case of monomeric CD, the first indication of the formation of the inclusion complex with βCD is a selective chemical shift variation of the H nuclei directly experiencing the void CD cavity. For PRX@D_2O, a downfield shift (deshielding) of H3 and H7 was observed.[46] In a similar way, HR-MAS NMR spectrum of PRX@CDNS presented in this work shows deshielding of H3 and H7 compared to the pure PRX@D_2O (compare Fig. 3a to Fig. 3b), consistent with the presence of a contribution of the inclusion complex to the magnetic environment of H3 and H7 of PRX entrapped in the CDNS in the CDNS. This finding is particularly interesting if compared with previous results on the encapsulation of ibuprofen in CDNS.[31] In that case, the NMR signals of racemic ibuprofen (IP) did not show the typical doubling of peaks due to the formation of diastereomeric inclusion complex with the homochiral monomeric cyclodextring, nor selective chemical shift variation compared to the reference in D_2O with monomeric CD. These results showed that IP was likely to interact with the polymeric backbone (voids I) without formation of genuine inclusion complexes IP-βCD (inclusion in voids II). In the present case, the selective complexation induced chemical shift seems to indicate at least a partial contribution of the

formation of inclusion complexes of PRX with voids II of the cyclodextrin units of CDNS to the overall drug-polymer interaction, though drug confinement in the polymeric pores (voids I) gives the major contribution to drug entrapment in the hydrogel.

PRX@D$_2$O and PRX@CDNS Dynamics

The dNMR experiments here reported explore the diffusion time range t_d (0.03-0.11) s. The experimental data are analysed following a procedure, proposed by some of us,[31] suitable to investigate the motion regime in a selected time window $t_{d(min)}$- $t_{d(max)}$. The method consists essentially of two steps: *i)* the linear regression of $\ln(I(q,t_d)/I_0)$ *vs* q^2 gives the MSD for each selected observation time according to eq. 4, the experimental data are shown in figure 4a). *ii)* the log-log plot of MSD vs t_d allows to obtain the diffusion exponent (eq. 5) as slope and D'(t_d=1) as intercept of the linear fit. The graph is reported in Figure 4b).

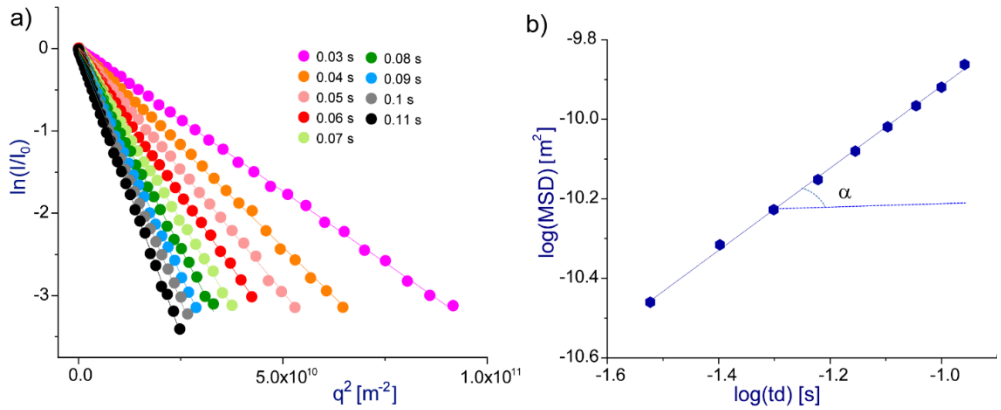

Figure 4. a) Normalized NMR signal decay $I(q,t_d)$ *vs* q^2 for PRX@CDNS. b) Log-log plot of means square displacements $< z_M^2 >$ as function of the observation time t_d. Line fitting the experimental data are also reported. All the experiments were performed at 305 K.

The analysis of PRX motion loaded in CDNS polymer matrix, following steps *i* and *ii*, gives an exponent α =1.03 (R^2=0.998). Accordingly, the drug dynamics follows the laws of ordinary

Fickian diffusion when encapsulated in the gel polymer matrix. The numerical value of the diffusion coefficient, calculated according to eq. 6, is reported in table 2 and it increases linearly with time.

The diffusion coefficient of PRX dissolved in water solution has been determined at different drug concentration with PGSE experiments at a single diffusion time Δ value and the results (using eq. 4) are also reported in table 2. The plot of *D* versus C_n (n=1-6) is shown in Figure 5.

Table 2. Diffusion coefficient *D* (m^2/s) of PRX@D_2O at variable concentration and PRX@CDNS. The *D* values are measured at 305 K.

Sample	$D \cdot 10^{-10}$ (m^2/s)
PRX@D_2O C_1	6.15
PRX@D_2O C_2	5.93
PRX@D_2O C_3	5.68
PRX@D_2O C_4	5.56
PRX@D_2O C_5	5.39
PRX@D_2O C_6	4.39
PRX@CDNS C_g	5.9

The diffusivity of PRX in solution decreases (from $6.15 \cdot 10^{-10}$ to $4.39 \cdot 10^{-10}$ m^2/s) with increasing drug concentration (C_1-C_6) due to the formation of various size aggregates in D_2O. A pictorial representation of the aggregation phenomenon of the drug in solution is shown in Figure 5.

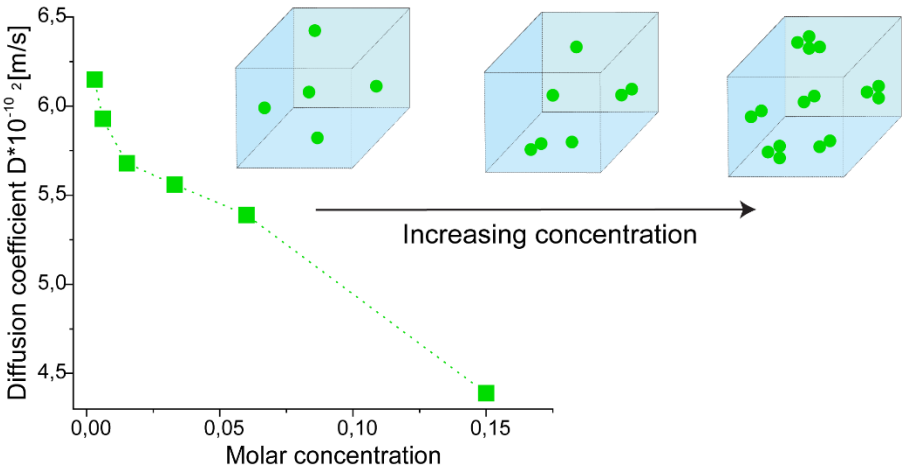

Figure 5. Plot of the diffusion coefficients *D* (m^2/s) *versus* C_n (n=1.6) for PRX@D_2O. A pictorial description of PRX aggregation in D_2O is also drawn. Green circles represent the PRX molecules.

It is important to note that the diffusion value of PRX loaded in CDNS at 0.15 M concentration (C_g) is comparable with the value found in D_2O for a lower concentration (C_2=0.006 M). These findings suggest that a double mechanism of solute-to-polymer adsorption and βCD encapsulation takes place in the hydrogel leading to a reduced concentration of free drug in solution. The HR-MAS spectrum (see Figure 3a) show well resolved lines with similar features to that in solution, thus indicating that adsorbed and free species are in fast exchange in the NMR timescale. Overall, PRX dynamics in CDNS nanoporous structure, although it remains Fickian over time, is determined by a drug-to-polymer adsorption phenomena. Similar behaviour was also found in the case of ethosuximide loaded in AC hydrogels, in that case polymer mesh size and drug concentration in gel phase has a relevant role in the adsorption process. A detailed mathematical model[34] has been developed using the experimental NMR data.

Release kinetics. In order to investigate the drug motion on a macroscopic time-scale and to characterize the release profile, we have performed *in vitro* release experiments on PRX-loaded hydrogels. The results are presented in Figure 6 together with mathematical fitting of the experimental data.

In general, the release profile is characterized by an initial release of a fraction of the drug absorbed called *burst release* and then by a well-defined kinetics[61] to maintain the effective drug concentration level. For PRX@CDNS, an initial burst release of 26 % was observed after 30 min., while 60 % of the drug is released by end of 8 h. The entire piroxicam release behavior over long time (shown in fig. 6a) is slow and even after 80 h is not complete. A comparison with literature data indicates that drug release kinetics from nanosponges often show a prolonged release profile over time. Previous in vitro studies showed that flurbiprofen (also a NAISD) was released slowly from β-CD nanosponges, with a percentage of almost 10% after 2 hours[12]. Similar results were obtained with acyclovir loaded in carboxylated nanosponges in which case a prolonged release rate without the initial burst effect was observed.[62]

The drug dissolution profile, f_t as a function of time, *t*, (*t*=0-8 h) is fitted using Higuchi and Korsmeyer-Peppas[63,64] power equations:

$$f_t = \frac{M_t}{M_\infty} = k_H t^{1/2} \quad (7)$$

$$f_t = \frac{M_t}{M_\infty} = k_{KP} t^n \quad (8)$$

where M_t and M_∞ are the cumulative amounts of drug released at time *t* and at infinite time, respectively; k_H (Higuchi constant) and k_{KP} (Korsmeyer-Peppas constant) are both related to the structural properties of the polymer matrix; n is a diffusional exponent, indicative of the solute transport mechanism. Accordingly, a value of $n \leq 0.45$ accounts for Fickian diffusion mechanism, $0.45<n<0.89$ for anomalous or non-fickian transport[65], n = 0.89 and n>0.89 for case

II transport, and super case II transport[60,66] respectively. The parameters resulting from fitting the first 60% of normalized drug release with Higuchi and Korsmeyer-Peppas models along with R^2 are collected in Table 3. The experimental release profile is well described by Korsmeyer−Peppas model (see fig. 6b) with a value of n=0.296, indicative of Fickian diffusion.

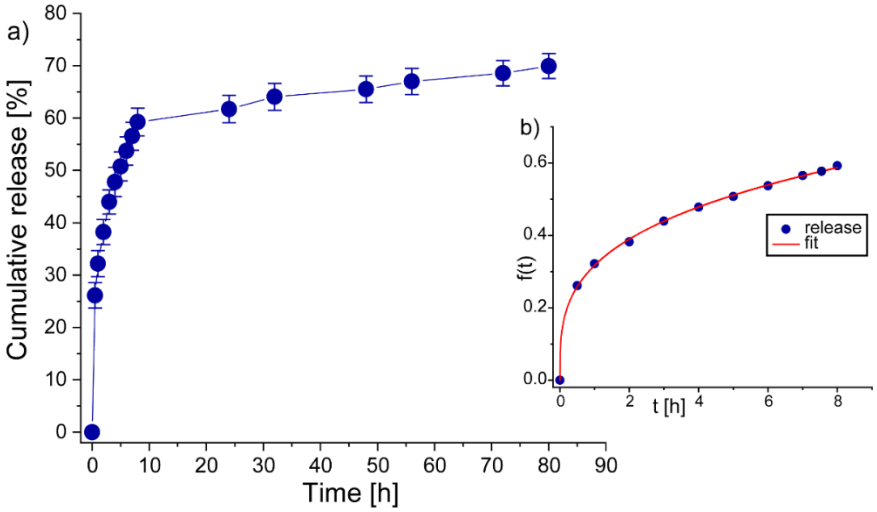

Figure 6. a) In vitro release profiles of piroxicam from CDNS in the time range (0-80) hours. b) Mathematical fit of piroxicam release against time (eq. 8) in the time range (0-8) hours, R^2=0.999. All of the errors are lower than 5%.

The diffusion coefficient D_R from the release data was calculated using a mathematical model based on mass balances, *i.e.* on fundamental conservation laws[34] for the two phases G = hydrogel, and S = solution. Diffusion through CDNS hydrogel can be described according to the second Fick's law with a 1-dimensional model in a cylindrical geometry, as shown in Eq. (9). Eqs. (10) and (11) represent the boundary conditions for the left and the right border, respectively. The first one implies profile symmetry at the center (that is, with respect to cylinder axis), while the second one represents the equivalence between the material diffusive fluxes at

the water/hydrogel surface. The radius (r) is the characteristic dimension for the investigated transport phenomenon.

$$\frac{\partial C_G}{\partial t} = D \cdot \frac{1}{r} \cdot \frac{\partial}{\partial r} \cdot \left(r \cdot \frac{\partial C_G}{\partial r} \right) \quad (9)$$

$$V_S \cdot \frac{\partial C_G}{\partial t} = k_C \cdot S_{exc} \cdot (C_G - C_S) \quad (10)$$

$$C_S(t = 0) = 0 \quad (11)$$

$$C_G(t = 0) = C_{G,0} = \frac{m_{G,0}}{V_G} \quad (12)$$

$$\left. \frac{\partial C_G}{\partial r} \right|_{r=0} = 0 \quad (13)$$

$$-D \cdot \left. \frac{\partial C_G}{\partial r} \right|_{r=R} = k_C \cdot (C_G - C_S) \quad (14)$$

where C_G is the mean drug concentration within the hydrogel, C_S the mean drug concentration in the outer solution, V_S the volume of the solution, V_G the hydrogel volume, m_G the drug mass present inside the matrix and S_{exc} the exchange interfacial surface, *i.e.* the boundary surface between gel and surrounding solution (the side surface).

Finally, the mass transfer coefficient k_c is computed through Sherwood number (*Sh*) according to the penetration theory with a totally isotropic diffusion in radial direction (eq. 15).

$$Sh = \frac{8}{\pi} = \frac{k_C \cdot 2r}{D_R} \quad (15)$$

The diffusion coefficient D_R resulting from fitting the release data (see Fig. SI3) is reported in Table 3. Interestingly, the value of the macro diffusion D_R is of the same order of magnitude of micro diffusion D_{NMR} in gel phase, thus indicating that the transition from micro to a macro time scale does not influence drug dynamics.

Table 3. Parameters (k_H, k_{KP}, n, D_R) obtained by fitting the drug release data with Higuchi and Korsmeyer−Peppas models. The diffusion coefficient of PRX in β-CDNS gel, obtained from NMR data, is also reported.

Higuchi		Korsmeyer-Peppas			D_R(PRX@CDNS) [m^2/s]	D_{NMR}(PRX@CDNS) [m^2/s]
k_H	R^2	k_{KP}	n	R^2	$3.1 \cdot 10^{-10}$	$5.9 \cdot 10^{-10}$
0.229	0.897	0.317	0.296	0.999		

The release behaviour is also indicative for mechanistic considerations. In CDNS hydrogel, the overall release process is characterised by two steps: *i*) a Korsmeyer-Peppas kinetics driven by Fickian diffusion of the drug on the polymer surface or through the water-filled nanosponge large pores (voids I) which accounts for the 60% of the release in 8 hours, *ii)* a steady state condition over a long time (80 hours) due to the release of an additional 10% of the drug encapsulated in the β-cyclodextrin NS small cavities, *i.e.* in the smaller pores of the crosslinked polymer backbone or via formation of genuine inclusion complex in the CD macrocycles (voids II). The ratio of two kinetics components is 6:1. Overall, CDNS hydrogel nanoarchitectonics enable sustained drug release through a dual functionality deriving from the concomitant swelling capacity of the hydrogels with the formation of large pores and from the drug-to-polymer adsorption together with complexation capability of the β-CDs moieties. A two-step release kinetics was also observed for ibuprofen loaded in silica xerogels.[67] The initial diffusion-controlled step was followed by a slower release rate (within 9 hours) due to the three-

dimensional silica network which effectively entrap the drug molecules. In our system PRX@CDNS, the interactions of PRX with the polymer network and/or drug-βCD complex formation are observed in the ^{1}H HR-MAS spectrum (section 3.2) and described in a previous theoretical study by Raffaini *et al*.[68]

CONCLUSIONS

This work reveals that β-cyclodextrin nanosponges crosslinked with PMDA hydrogels are good candidates for the controlled delivery of piroxicam drug and the procedure can potentially be extended to other types of small molecules confined in porous polymer systems. The dynamics of the small molecules loaded in the hydrogel, described by HR-MAS dNMR data and by the release profile, follows in both cases Fick's laws with a diffusion coefficient constant over time.

The macroscopic release kinetics shows a two-stage mechanism, the first is diffusion driven according to Korsmeyer-Peppas model for about the 60% of the release. In the second step, a prolonged release over time is observed due to the slow release of PRX encapsulated within the β-cyclodextrin cavities. The CDNS polymer nanoarchitectonics has a relevant dual effect on the sustained drug release. Furthermore, these results indicate the capability of HR-MAS dNMR technique to elucidate the drug-polymer interaction mechanism and predict the macroscopic release dynamics of small drugs encapsulated in CDNS-based hydrogels.

ASSOCIATED CONTENT

The Supporting Information is available online.

Solution NMR spectra of piroxicam; NMR dynamics of H_2O in βCDNS hydrogel.

Mathematical fit of release data.

AUTHOR INFORMATION

Corresponding Author

* Corresponding author, Franca Castiglione, Department of Chemistry, Materials and Chemical Engineering “G. Natta”, Politecnico di Milano, Piazza L. da Vinci 32, 20133 Milano, Italy. E-mail: franca.castiglione@polimi.it

Author Contributions

The manuscript was written through contributions of all authors. All authors have given approval to the final version of the manuscript.

CONFLICT OF INTEREST

The authors declare no conflict of interest.

REFERENCES

(1) Szejtli, J. Introduction and general overview of cyclodextrin chemistry. *Chem. Rev.* **1998**, 98, 1743−1753.

(2) Szejtli, J. Cyclodextrin Technology. **1988**, Springer Netherlands.

(3) Bilensoy, E. Cyclodextrins in pharmaceutics, cosmetics, and biomedicine: current and future industrial applications. **2011**, John Wiley and Sons Inc., Singapore.

(4) Trotta, F.; Mele, A. Nanosponges: synthesis and applications. Weinheim, Germany: Wiley-VCH, **2019**, 1-336.

(5) Sherje, A. P.; Dravyakar, B. R.; Kadam, D.; Jadhav, M. Cyclodextrin-based nanosponges: A critical review. *Carbohydrate Polymers* **2017**, *173*, 37-49.

(6) Trotta, F.; Tumiatti, W. and Vallero, R. Nanospugne a base di ciclodestrine funzionalizzate con gruppi carbossilici: sintesi e utilizzo nella decontaminazione da metalli pesanti e composti organici. Italian Patent no. A000614, MI, **2004**.

(7) Caldera, F.; Tannousa, M.; Cavalli, R.; Zanetti, M.; Trotta, F. Evolution of Cyclodextrin Nanosponges. *International Journal of Pharmaceutics* **2017**, *531*, 470-479.

(8) Shende, P.; Desai, D.; Gaud, R. S. Hybrid Nanosponges: From Fundamentals to Applications. Wiley Online Library, **2019**, 173–192.

(9) Cavalli, R.; Akhtera, A. K.; Bisazzaa, A.; Giustetto, P.; Trotta, F.; Vaviac, P. Nanosponge formulations as oxygen delivery systems. *International Journal of Pharmaceutics* **2010**, *402*, 254-257.

(10) Tejashri, G.; Amrita, B.; Darshana, J. Cyclodextrin based nanosponges for pharmaceutical use: a review. *Acta Pharm*. **2013**, *63*, 335-358.

(11) Allahyari, S.; Trotta, F.; Valizadeh, H.; Jelvehgari, M.; Zakeri-Milani, P. Cyclodextrin-based nanosponges as promising carriers for active agents, *Expert Opinion on Drug Delivery* **2019**, *16*, 467-479.

(12) Cavalli, R.; Trotta, F.; Tumiatti, V. Cyclodextrin-based nanosponges for drug delivery. *J. Incl. Phenom. Macrocycl. Chem.* **2006**, *56*, 209-213.

(13) Mendes, C.; Meirelles, G. C.; Barp, C. G.; Assreuy, J.; Silva, M. A. S.; Ponchel, G. Cyclodextrin based nanosponge of norfloxacin: Intestinal permeation enhancement and improved antibacterial activity.*Carbohydrate Polymers* **2018**, *195*, 586–592.

(14) Trotta, F.; Cavalli, R. Characterization and applications of new hyper-crosslinked cyclodextrins. *Compos. Interfaces* **2009**, *16*, 39–48.

(15) Castiglione, F.; Crupi, V.; Majolino, D.; Mele A.; Rossi, B.; Trotta, F.; Venuti, V. Vibrational spectroscopy investigation of swelling phenomena in cyclodextrin nanosponges. *J. Raman Spectrosc.* **2013**, *44*, 1463–1469.

(16) Rossi, B.; Paciaroni, A.; Venuti, V.; Fadda, G. C.; Melone, L.; Punta, C.; Crupi, V.; Majolino, D. and Mele, A. SANS investigation of water adsorption in tunable cyclodextrin-based polymeric hydrogels. *Phys. Chem. Chem. Phys*. **2017**, 19, 6022-6029.

(17) Crupi, V.; Fontana, A.; Majolino, D.; Mele, A.; Melone, L.; Punta, C.; Rossi, B.; Rossi, F.; Trotta, F; & Venuti ,V. Hydrogen-bond dynamics of water confined in cyclodextrin nanosponges hydrogel. *J. Incl. Phenom. Macrocycl. Chem.* **2014**, *80*, 69–75.

(18) van de Manakker, F.; Vermonden, T.; van Nostrum C. F.; and Hennink, W. E. Cyclodextrin-based polymeric materials: synthesis, properties, and pharmaceutical/biomedical applications. *Biomacromolecules* **2009**, *10*, 3157-3175.

(19) Izawa, H.; Kawakami, K.; Sumita, M.; Tateyama, Y.; Hill, J. P. and Ariga, K. β-Cyclodextrin-crosslinked alginate gel for patient-controlled drug delivery systems: regulation of host–guest interactions with mechanical stimuli. *J. Mater. Chem. B* **2013**, *1*, 2155-2161.

(20) Zhang, Y. S.; and Khademhosseini, A. Advances in engineering hydrogels. *Science* **2017**, *356*, eaaf3627.

(21) Culver, H. R.; Clegg, J. R.; Peppas, N. A. Analyte-responsive hydrogels: intelligent materials for biosensing and drug delivery. *Acc. Chem. Res.* **2017**, *50*, (2), 170-178.

(22) Ma, C.; Shi, Y.; Pena, D. A.; Peng, L.; Yu, G. Thermally responsive hydrogel blends: a general drug carrier model for controlled drug release. *Angew. Chem. Int. Ed.* **2015**, *54*, 7376-7380.

(23) Zhu, J.; Zhang, X.; Qin, Z.; Zhang, L.; Ye, Y.; Cao, M.; Gao, L.; Jiao, T. Preparation of PdNPs doped chitosan-based composite hydrogels as highly efficient catalysts for reduction of 4-nitrophenol. *Colloids and Surfaces A: Physicochemical and Engineering Aspects* **2021**, *611*, 125889

(24) Song, J.; Yuan, C.; Jiao, T.; Xing, R.; Yang, M.; Adams, D.J.; and Yan, X. Multifunctional antimicrobial biometallohydrogels based on amino acid coordinated self-assembly. *Small* **2021**, *16*, 1907309.

(25) Xing, R.; Liu, K.; Jiao, T.; Zhang, N.; Ma, K.; Zhang, R.; Zou, Q.; Ma, G.; Yan, X. An injectable self-assembling collagen–gold hybrid hydrogel for combinatorial antitumor photothermal/photodynamic therapy *Adv. Mater.* **2016**, *28*, 3669-3676.

(26) Li, J. and Mooney, D. J. Designing hydrogels for controlled drug delivery. *Nature Reviews Materials* **2016**, *1*, 1-17.

(27) Rossi, F.; Ferrari, R.; Castiglione, F.; Mele, A.; Perale, G.; Moscatelli, D. Polymer hydrogel functionalized with biodegradable nanoparticles as composite system for controlled drug delivery. *Nanotechnology* **2015**, *26*, Article number 015602.

(28) Lin, C.-C.; Metters, A. T. Hydrogels in controlled release formulations: Network design and mathematical modelling. *Advanced Drug Delivery Reviews* **2006**, *58*, 1379–1408.

(29) Ferreira, J. A.; Grassi, M.; Gudiño, E.; de Oliveira, P. A new look to non-Fickian diffusion. *Appl. Math. Model*. **2015**, *39*, 194-204.

(30) Wang, B.; Kuo, J.; Bae S. C. and Granick, S. When Brownian diffusion is not Gaussian. *Nature Mat.* **2012**, *11*, 481-485.

(31) Ferro, M.; Castiglione, F.; Punta, C.; Melone, L.; Panzeri, W.; Rossi, B.; Trotta, F. and Mele, A. Anomalous diffusion of Ibuprofen in cyclodextrin nanosponges hydrogels: an HRMAS NMR study. *Beilstein J. Org. Chem*. **2014**, *10*, 2580-2593.

(32) Castiglione, F.; Casalegno, M.; Ferro, M.; Rossi, F.; Raos, G. and Mele, A. Evidence of superdiffusive nanoscale motion in anionic polymeric hydrogels: Analysis of PGSE- NMR data and comparison with drug release properties. *J. Controlled Release* **2019**, *305*, 110-119.

(33) Karger, J. and Ruthven, D. M. Diffusion in nanoporous materials: fundamental principles, insights and challenges. *New J. Chem*. **2016**, *40*, 4027-4048.

(34) Rossi, F.; Castiglione, F.; Ferro, M.; Marchini, P.; Mauri, E.; Moioli, M.; Mele, A. and Masi, M. Drug-Polymer interactions in hydrogel-based drug delivery systems: experimental and theoretical study. *Chem. Phys. Chem*. **2015**, *16*, 2818-2825.

(35) Rossi, F.; Castiglione, F.; Ferro, M.; Moioli, M.; Mele A. and Masi, M. The role of drug–drug interactions in hydrogel delivery systems: experimental and model study. *Chem. Phys. Chem*. **2016**, *17*, 1-9.

(36) Perale, G.; Rossi, F.; Santoro, M.; Marchetti, P.; Mele, A.; Castiglione, F.; Raffa, E.; Masi, M. Drug release from hydrogel: a new understanding of transport phenomena. *J. Biomed. Nanotechnol*. **2011**, *7*, 476-481.

(37) Higuchi, W.I. Diffusional models useful in biopharmaceutics. *J. Pharm. Sci*. **1967**, *56*, 315-324.

(38) Siepmann, J. and Peppas, N. A. Higuchi equation: Derivation, applications, use and misuse. *Int. J. Pharm*. **2011**, *418*, 6-12.

(39) Siepmann, J.; Siepmann, F. Modeling of diffusion controlled drug delivery. *J. Control Release* **2012**, *161*, 351-362.

(40) Caccavo, D.; Cascone, S.; Lamberti, G. and Barba, A. A. Modeling the drug release from hydrogel-based matrices. *Mol. Pharmaceutics* **2015**, *12*, 474-483.

(41) Tokuyama, H.; Nakahata, Y.; Ban, T. Diffusion coefficient of solute in heterogeneous and macroporous hydrogels and its correlation with the effective crosslinking density. *Journal of Membrane Science* **2020**, *595*, 117533.

(42) Masaro, L.; Zhu, X. X. Physical models of diffusion for polymer solutions, gels and solids. *Prog. Polym. Sci*. **1999**, *24*, 731–775.

(43) Fujita, H. Diffusion in polymer-diluent systems. *Adv. Polym. Sci*. **1961**, *3*, 1-47.

(44) Cukier, R. I., Diffusion of Brownian Spheres in Semidilute Polymer Solutions. *Macromolecules* **1984**, *17*, 252-255.

(45) Fatin-Rouge, N.; Milon, A.; Buffle, J.; Goulet, R. R.; Tessier, A. Diffusion and partitioning of solutes in agarose hydrogels: The relative influence of electrostatic and specific interactions. *J. Phys. Chem. B* **2003**, *107*, 12126–12137.

(46) Fronza, G.; Mele, A.; Redenti, E. and Ventura, P. Proton Nuclear Magnetic Resonance Spectroscopy Studies of the Inclusion Complex of Piroxycam with β-Cyclodextrin. *J. Pharm. Sci*. **1992**, *81*, 1162-1165.

(47) Venuti, V.; Rossi, B.; Mele, A.; Melone, L.; Punta, C.; Majolino, D.; Masciovecchio, C.; Caldera, F.; Trotta, F. Tuning structural parameters for the optimization of drug delivery performance of cyclodextrin based nanosponges. *Expert Opin. Drug Deliv.* **2017**, *14*, 331–340.

(48) Zubkov, M.; Dennis, G. R.; Stait-Gardner, T.; Torres, A. M.; Willis, S. A.; Zheng, G. and Price, W. S. Physical characterization using diffusion NMR spectroscopy. *Magn. Reson. Chem.* **2017**, *55*, 414–424.

(49) Phillies, G. Diffusion on a molecular scale as observed using PGSE NMR. *Concepts in Magnetic Resonance Part A* **2015**, *44*, 1-15.

(50) Evans, R. The interpretation of small molecule diffusion coefficients: Quantitative use of diffusion-ordered NMR spectroscopy. *Progress in Nuclear Magnetic Resonance Spectroscopy* **2020**, *117*, 33–69.

(51) Fiorati, A.; Negrini, N. C.; Baschenis, E.; Altomare, L.; Faré, S.; Schieroni, A. G.; Piovani, D.; Mendichi, R.; Ferro, M.; Castiglione, F.; Mele, A.; Punta, C.; Melone, L. TEMPO-nanocellulose/Ca^{2+} hydrogels: Ibuprofen drug diffusion and in vitro cytocompatibility. *Materials* **2020**, *13*, 183-199.

(52) Kimmich, R. Principles of Soft-Matter Dynamics. Springer: New York, **2015**, 1-656.

(53) Rossi, F.; Rainer A. Nanomaterials for Theranostics and Tissue Engineering. Elsevier, **2020**, 83-105.

(54) Castiglione, F.; Crupi, V.; Majolino, D.; Mele, A.; Rossi, B.; Trotta, F. and Venuti, V. *J. Phys. Chem. B*, **2012**, *116*, 13133-13140.

(55) Metzler, R.; Klafter, J. The random walk's guide to anomalous diffusion: a fractional dynamics approach. *Phys. Rep.* **2000**, *339*, 1–77.

(56) Fan, Y. and Gao, J.-H. Fractional motion model for characterization of anomalous diffusion from NMR signals. *Phys. Rev. E* **2014**, *92*, 012707.

(57) Moin, A.; Roohi, N. K. F.; Rizvi, S. M. D.; Ashraf, S. A.; Siddiqui, A. J.; Patel, M.; Ahmed, S. H.; Gowda, D. V. and Adnan, M. Design and formulation of polymeric nanosponge tablets with enhanced solubility for combination therapy. *RSC Adv.* **2020**, *10*, 34869-34884.

(58) Mishra, B. K.; Arey, J. S.; Sathyamurthy, N. Stacking and spreading interaction in N-heteroaromatic systems. *J Phys Chem*. **2010**, *114*, 9606-9616.

(59) Lee, E. C.; Kim, D.; Jurecka, P.; Tarakeshwar, P.; Hobza, P.; Kim, K. S. Understanding of assembly phenomena by aromatic−aromatic interactions: benzene dimer and the substituted systems. *J Phys Chem A* **2007**, *111*, 3446-3457.

(60) Djimant, D.; Djimant, L. N. and Veselkov, A. N. ^{1}H NMR investigation of self-association of aromatic drug molecules in aqueous solution. Structural and thermodynamical analysis. *Journal of Chemical Society, Faraday Transactions* **1996**, *92*, 383–390.

(61) Ritger, P. L.; Peppas, N. A. A simple equation for description of solute release II. Fickian and anomalous release from swellable devices. *Journal of Controlled Release*, **1987**, *5*, 37-42.

(62) Lembo, D.; Swaminathan, S.; Donalisio, M.; Civra, A.; Pastero, L.; Aquilano, D.; Vavia, P.; Trotta, F.; Cavalli. R. *Int. J. Pharm*. **2013**, *443*, 262– 272.

(63) Korsmeyer, R.W.; Gurny, R.; Doelker, E.; Buri, P. and Peppas, N. A. Mechanisms of solute release from porous hydrophilic polymers. *Int. J. Pharm*. **1983**, *15*, 25-35.

(64) Peppas, N. A.; Narasimhan, B. Mathematical models in drug delivery: How modeling has shaped the way we design new drug delivery systems. *J. Control Release* **2014**, *190*, 75-81.

(65) Peppas, N.A. Analysis of Fickian and non-Fickian drug release from polymers. *Pharm. Acta Helv*. **1985**, *60*, 110–111.

(66) Fu, Y.; Kao, W. J. Drug release kinetics and transport mechanisms of non-degradable and degradable polymeric delivery systems. *Expert Opin Drug Deliv*. **2010**, *7*, 429–44.

(67) Czarnobaj, K. Preparation and characterization of silica xerogels as carriers for drugs. *Drug Delivery* **2008**, *15*, 485-492.

(68) Raffaini, G. and Ganazzoli, F. Understanding surface interaction and inclusion complexes between piroxicam and native or crosslinked β-cyclodextrins: the role of drug concentration. *Molecules* **2020**, *25*, 2848.

TOC